

## Case Report

# Smooth muscle hamartoma of the lungs in a Wistar Hannover rat

Shinya Miyazaki<sup>1\*</sup>, Chinatsu Fujiwara<sup>1</sup>, Yoshitaka Katoh<sup>1</sup>, Tsuyoshi Ito<sup>1</sup>, Aya Koyama<sup>1</sup>, Naofumi Takahashi<sup>1</sup>, Atsushi Shiga<sup>1</sup>, and Takanori Harada<sup>1</sup>

<sup>1</sup> The Institute of Environmental Toxicology, 4321 Uchimoriya-machi, Joso-shi, Ibaraki 303-0043, Japan

**Abstract:** Hamartomas are tumor-like masses comprising disorganized normal tissue elements. To date, spontaneous hamartomas have been reported in several organs and tissues in rodents but not in the lungs. Here, we report the first case of a hamartoma in the lungs of a 108-week-old female Wistar Hannover rat. Grossly, a white spot, 7 mm in diameter, was observed on the costal surface of the left lung. Histopathologically, the nodular lesions adjacent to the bronchioles comprised mature smooth muscle cells. The lesion was not encapsulated and spread along the alveolar walls and ducts without compression of the surrounding tissue. In the nodules, elastic fibers enclosed small lumens lined with factor VIII-related antigen-positive endothelial cells. This structure suggested that the nodule mimicked an artery. Moreover, structural abnormalities were observed within the bronchioles and arterioles owing to the increased number of smooth muscle cells in the surrounding tissues. These features suggested that this was a case of tissue malformation rather than a neoplasm, leading to the diagnosis of a smooth muscle hamartoma of the lung. (DOI: 10.1293/tox.2023-0056; J Toxicol Pathol 2023; 36: 193–198)

**Key words:** smooth muscle hamartoma, malformation, lung, rat, Wistar Hannover

Hamartomas are tumor-like masses comprising disorganized normal tissue elements that can occur at any location<sup>1, 2</sup>. In rodents, spontaneous hamartomas have been reported in several organs and tissues including the skin, brain, small intestine, and uterus, but not in the lungs<sup>3–6</sup>. In domestic animals, however, several cases of pulmonary hamartoma have been reported<sup>7, 8</sup>. They are sequestered from the normal airways and contain excessive amounts of alveolar tissues. In humans, pulmonary hamartomas are typically characterized as benign neoplasms rather than tissue malformations caused by clonal chromosomal mutations<sup>9, 10</sup>. It is a well-circumscribed mass composed of two or more types of mesenchymal tissues and epithelium, with cartilaginous tissue being the most frequently observed mesenchymal tissue<sup>10, 11</sup>. Moreover, pulmonary fibroleiomyomatous hamartomas, which mainly consist of smooth muscles and connective tissues, have been previously reported<sup>12–14</sup>. In this study, we describe the first case of hamartoma occurring in the lungs of a Wistar-Hannover rat and compare its histopathological features with those of a human pulmonary hamartoma.

A specific pathogen-free female Wistar Hannover rat

[Br/Han:WIST@Jcl (GALAS)], purchased from the Fujiyama Breeding Center, CLEA Japan Inc. (Shizuoka, Japan), was used in a combined chronic toxicity and carcinogenicity study as part of the middle-dose group. The animal was housed in a wire-mesh stainless steel cage in a barrier-sustained animal room controlled at a temperature of  $22 \pm 2$  °C; humidity of  $50 \pm 20\%$ ; ventilation for 10 times or more per hour, and illumination for 12 h/day. Pulverized MF Mash (Oriental Yeast Co., Ltd., Tokyo, Japan) and tap water were provided *ad libitum*. The animal was handled in testing facilities accredited by AAALAC International in accordance with the Animal Care and Use Program of the Institute of Environmental Toxicology (approval No. AC16060).

The animals were euthanized under isoflurane anesthesia and necropsied because of the deterioration of their condition at 108 weeks of age, which turned out to be due to spontaneous pituitary adenoma. Necropsy revealed a white spot, 7 mm in diameter on the costal surface of the caudal end of the left lung. This macroscopic lesion was considered a spontaneous lesion because there was no dose-response relationship between the lesion and treatment. The lung was fixed in 10% neutral-buffered formalin following the instillation of fixative through the trachea, embedded in paraffin wax, and sectioned at 4  $\mu\text{m}$  of thickness. Sections were subjected to hematoxylin and eosin (H&E) and Elastica Van Gieson (EVG) staining. Immunohistochemistry was performed using antibodies against S-100 (1:400),  $\alpha$ -smooth muscle actin ( $\alpha$ -SMA) (1A4, 1:100), desmin (D33, prediluted), factor VIII-related antigen (FVIII-RAG) (prediluted), and proliferating cell nuclear antigen (PCNA) (PC10, 1:5,000). The dilution ratios were based on the data from

Received: 14 April 2023, Accepted: 23 June 2023

Published online in J-STAGE: 7 July 2023

\*Corresponding author: S Miyazaki (e-mail: s.miyazaki@iet.or.jp)

©2023 The Japanese Society of Toxicologic Pathology

This is an open-access article distributed under the terms of the Creative Commons Attribution Non-Commercial No Derivatives

(by-nc-nd) License. (CC-BY-NC-ND 4.0: <https://creativecommons.org/licenses/by-nc-nd/4.0/>).



the database<sup>15</sup>. All primary antibodies except anti-FVIII-RAg were purchased from Dako (Agilent, Santa Clara, CA, USA). The anti-FVIII-RAg antibody was purchased from BioGenex Laboratories (Fremont, CA, USA). Antigen retrieval for PCNA and FVIII-RAg immunostaining assays were performed using a microwave at 98 °C with a citrate buffer (pH 6.0) for 5 min and proteinase K treatment (Dako) at 20 °C for 15 min, respectively. For the other antibodies except for the anti- $\alpha$ -SMA antibody, samples were autoclaved at 121 °C with a citrate buffer (pH 6.0) for 5 min as part of antigen retrieval. Antigen retrieval was not performed for  $\alpha$ -SMA immunostaining. Blocking was performed using 4% Block Ace (DS Pharma Biochemical, Osaka, Japan) at 20 °C for 30 min, followed by incubation with the primary antibodies at 4 °C overnight. Subsequently, sections were incubated with EnVision+System-HRP anti-mouse or anti-rabbit (Dako) secondary antibodies at 37 °C for 30 min. Positive reactions were visualized using 3,3-diaminobenzidine solution (Wako Pure Chemical Industries, Osaka, Japan) and nuclei were stained with Gill's hematoxylin. An area without lung lesions was used as the control tissue. Good reactivity was achieved without nonspecific reactions.

Corresponding to the macroscopic white spots in the lungs, the nodular lesion consisted of bundles of eosinophilic spindle cells running in a convoluted manner adjacent to the bronchioles. The nodule was not encapsulated and spread along the alveolar walls and ducts without compression of the surrounding tissues (Fig. 1A). Eventually, the nodule merged into the lamina propria and the muscle layer of the bronchioles. The spindle cells forming the lesion had mature nuclei with short to long fusiform and abundant eosinophilic cytoplasm, including a high frequency of cytoplasmic vacuoles (Fig. 1B). Some had large intracytoplasmic vacuoles that compressed the nuclei. The cells were well differentiated and showed no nuclear atypia or mitosis. Moreover, bundles of spindle cells often concentrically enclosed other bundles in the alveolar walls (Fig. 1C). Moreover, the wall of the arteriole near the nodule was partially thickened owing to spindle cell accumulation (Fig. 1D).

EVG staining revealed a circular arrangement of elastic fibers in the nodule and structure, with bundles of spindle cells concentrically enclosing another (Fig. 2A, 2B). Additionally, the number of spindle cells increased between the elastic fibers and epithelial cells of the bronchioli, which were connected to the nodule (Fig. 2C). It was also increased in the arteriolar subendothelium, causing partial wall thickening (Fig. 2D).

Immunohistochemically, all spindle cells were strongly positive for  $\alpha$ -SMA (Fig. 3A) and desmin but negative for S-100. The cells containing large intracytoplasmic vacuoles were positive for  $\alpha$ -SMA. FVIII-RAg immunostaining demonstrated the presence of endothelial cells lining the small lumen in the center of the elastic fiber ring, as revealed by EVG staining (Fig. 3B). However, similar positive reactions for FVIII-RAg were not observed in the structures in which the bundles of spindle cells were concentrically enclosed. PCNA positivity was rarely observed within the nodules,

including the spindle cells (Fig. 3C).

Based on their histopathological and immunohistochemical characteristics, spindle cells, including those with large intracytoplasmic vacuoles, were mature or degenerated smooth muscle cells. In this case, the structure of the nodule, in which elastic fibers and smooth muscle cells enclosed the lumen lined by FVIII-RAg-positive cells, resembled that of arteries. Moreover, the structure of the bundles of spindle cells concentrically enclosing another also mimicked the arteries. The lesion was accompanied by structural anomalies in the surrounding alveoli, bronchioli, and arterioles owing to partially increased smooth muscle cells in the subepithelium or subendothelium. Therefore, the lesion was considered a malformation of smooth muscle cells in the lung and was suspected to be a smooth muscle hamartoma.

For the differential diagnosis, leiomyoma, leiomyosarcoma, and smooth muscle hyperplasia were considered because the lesions mostly consisted of smooth muscle cells. In this case, the nodule resembled an artery-like structure with no neoplastic features such as encapsulation or compression of surrounding tissues, frequent mitosis, and nuclear atypia. In addition, vascular lesions such as proliferation of the endothelium and wrinkling of the arterial walls, suggestive of pulmonary hypertension that can induce smooth muscle hyperplasia, were not observed<sup>16, 17</sup>. Additionally, structural abnormalities were detected in the surrounding tissues, including ectopic smooth muscle cells in unusual locations. Therefore, this case was diagnosed as a smooth muscle hamartoma of the lung, given the development of a tumor-like malformed tissue as a result of the overgrowth of disorganized mature tissues or cells<sup>1, 2</sup>.

In humans, pulmonary hamartoma is recognized as a true benign mesenchymal neoplasm caused by clonal chromosomal mutations, according to the World Health Organization Classification of lung tumors due to clonal chromosomal mutations<sup>9, 10</sup>, despite the use of the term, hamartoma. The tumor is composed of two or more types of mesenchymal tissues and entrapped ingrown bronchial epithelium. Hyaline cartilage is the main element of the tumor which also contains fat, smooth muscle, or spindle cell-producing mucus<sup>10, 11</sup>. As a rare variant of pulmonary hamartoma, a pulmonary fibroleiomyomatous hamartoma has also been reported<sup>12-14</sup>. Histopathologically, it is a well-circumscribed mass resulting from the proliferation of smooth muscle cells and cuboidal respiratory epithelium extending into the alveolar septa. Pulmonary fibroleiomyomatous hamartomas are similar to pulmonary hamartomas, except that they lack cartilage and often present with multiple lesions. Kato *et al.* have reported that fibroleiomyomatous hamartomas are characterized by a polyclonal pattern; therefore, their histogenesis is unknown<sup>13</sup>. In the present case, the lesion was not encapsulated and the boundaries were unclear. It comprised only one element, smooth muscle, which forms artery-like structures and causes structural abnormalities in the arterioles and bronchioli. Additionally, the lesion was lined with alveolar epithelium. These features suggest that this lesion is distinct from human pulmonary hamartoma and fibro-



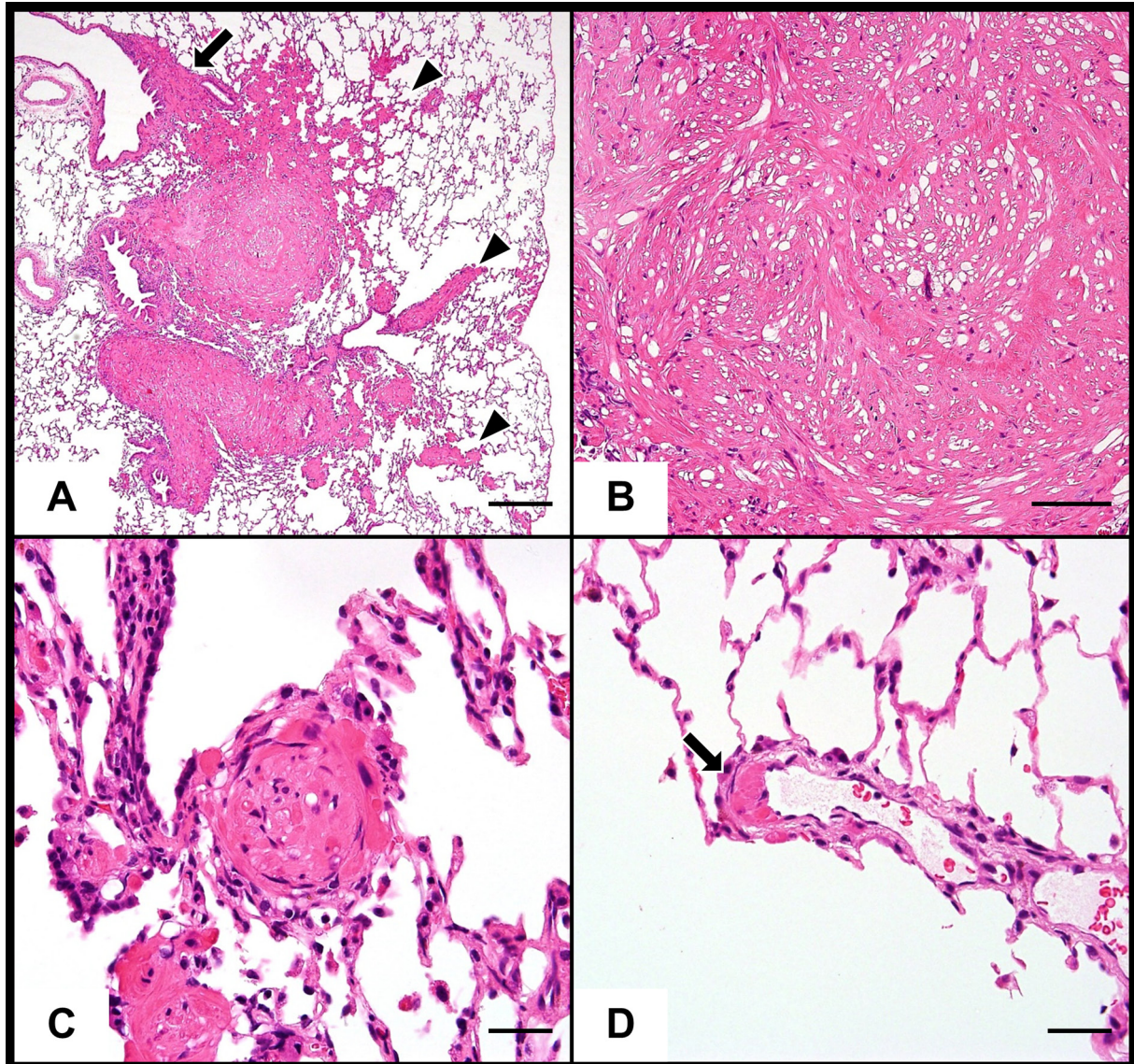


**Fig. 1.** The white spots in the lungs were stained with hematoxylin and eosin. A nodular lesion comprising bundles of eosinophilic spindle cells is observed adjacent to the bronchioles. The nodule is not encapsulated and spread along the alveolar walls and ducts (arrowheads) without compression of the surrounding tissues and merges into the lamina propria and muscle layer of the bronchioles (arrow) (A). Spindle cells have short-to-long fusiform mature nuclei and abundant eosinophilic cytoplasm, which often includes vacuoles. The cells show no atypia of nuclei (B). Bundles of spindle cells concentrically enclosing another bundle are observed in some alveolar walls (C). The wall of the arteriole near the nodule is partially thickened by the accumulation of spindle cells (arrow) (D). Bars indicate 200  $\mu\text{m}$  (A), 50  $\mu\text{m}$  (B), and 20  $\mu\text{m}$  (C and D).

leiomyomatous hamartoma and that this case was a malformation rather than a neoplasm, although its clonality was not analyzed. To distinguish this case from the well-known human pulmonary hamartoma, which is recognized as a benign neoplasm, we avoided using the term, pulmonary hamartoma, for diagnosis<sup>10</sup>. However, the term hamartoma has been preferentially used in veterinary pathology for malformations<sup>5</sup>. In this case, smooth muscle cells increased not only in the vasculature but also in the bronchioles and alveolar septa. Therefore, we diagnosed this case as a smooth muscle hamartoma of the lung based on the increase in the number of smooth muscle cells in several components. In

humans, smooth muscle hamartoma is a benign proliferation of smooth muscle cells that are mainly derived from the arrector pili muscle in the dermis<sup>18, 19</sup>. A similar lesion has been reported in dogs as a hamartoma of the arrector pili muscles<sup>20</sup>. These lesions consist of randomly oriented bundles of mature smooth muscle cells without encapsulation or compression, unlike neoplastic lesions. Although our case occurred in the lung, it had the same features such as bundles of mature smooth muscle cells, nonencapsulation, and no compression, resulting in the diagnosis of smooth muscle hamartoma of the lung. To the best of our knowledge, similar lesions forming artery-like structures in hu-



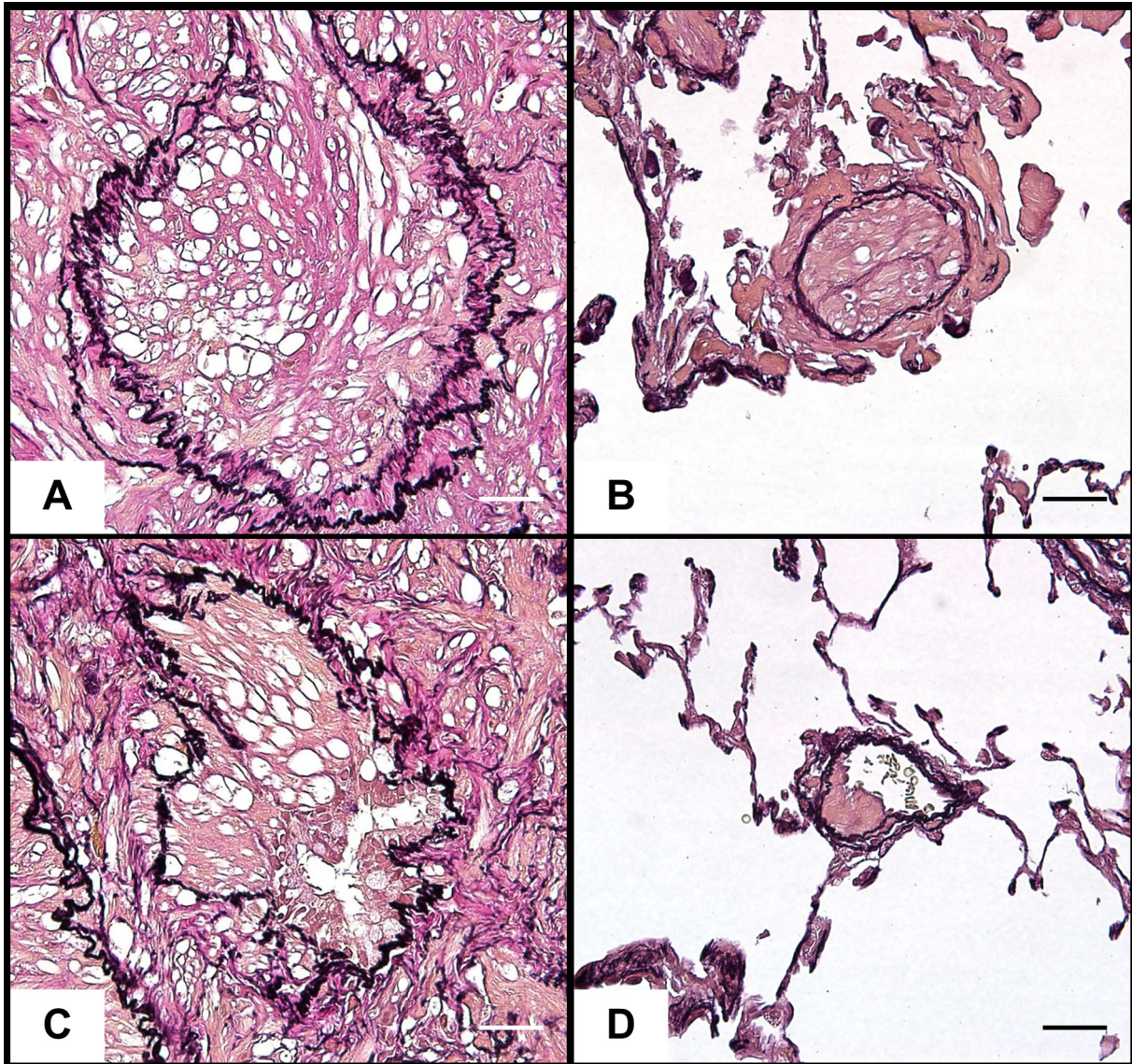


**Fig. 2.** Elastica Van Gieson (EVG) staining reveals the circular arrangement of elastic fibers in the nodule (A). The elastic fibers are also observed in the bundles of spindle cells concentrically enclosing another one (B). The spindle cells are increased between elastic fibers and epithelial cells of the bronchi which connect with the nodule (C). The spindle cells are also increased in the sub-endothelium of the arteriolar wall resulting in partial thickening of it (D). All figures show EVG staining. All bars indicate 20  $\mu$ m.

mans and other animals have not yet been reported.

Embryologically, the lungs develop as lung primordia derived from the foregut branching off into the interstitial tissue, which gives rise to the pulmonary blood vessels and smooth muscles of the bronchioles and alveolar septa. Pulmonary arteries develop by branching off parallel to the airways and delivering blood to the capillary network of the alveoli<sup>21, 22</sup>. In the present case, the lesion was located adjacent to the airways, where there is a pulmonary artery. This suggests that the smooth muscle cells of the lesion may have originated from the pulmonary arterial wall. Although a major part of the lesion formed artery-like structures, it contained smooth muscle anomalies, not only in the blood ves-

sels but also in the bronchioles and alveolar septa. In other words, the smooth muscle cells of the lesion originated from two components—blood vessels and airways. Therefore this lesion might occur in an early stage of pneumogenesis before the direction of differentiation of the smooth muscle cells branches off.

In conclusion, we report the first case of hamartoma resulting from an increase in smooth muscle cells in more than one component of the rat lungs. This may have occurred during the early stages of pneumogenesis. To distinguish them from human pulmonary hamartomas, we diagnosed this case as a smooth muscle hamartoma of the lung.



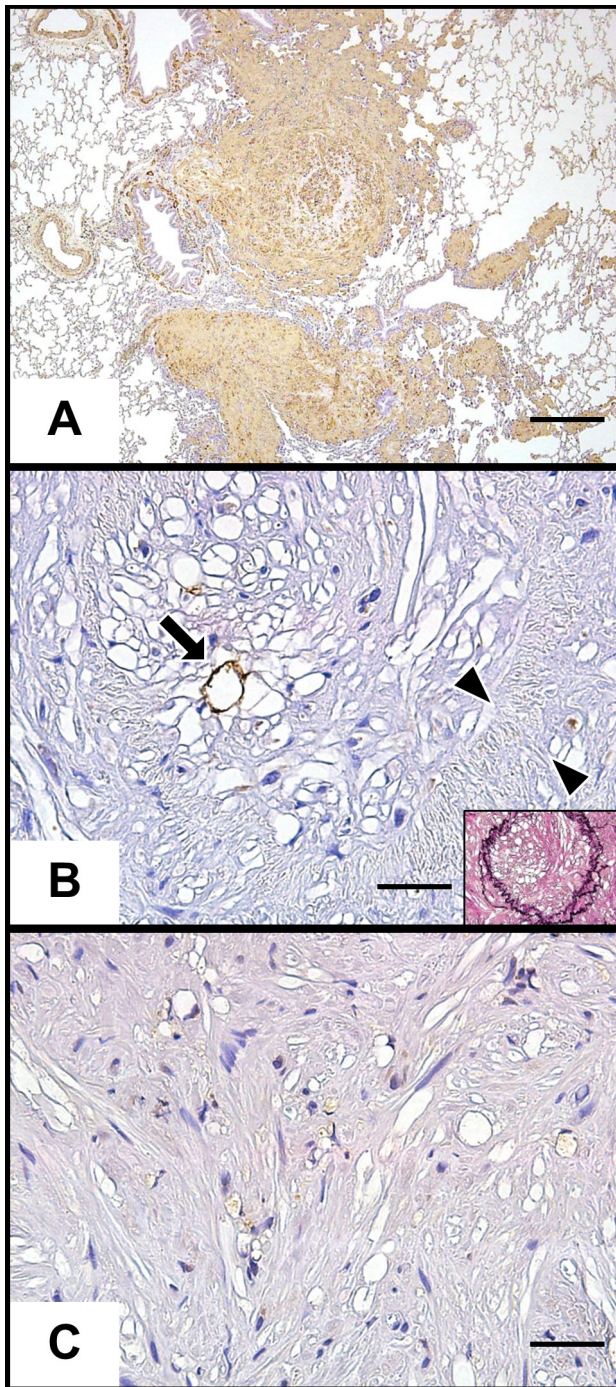


**Fig. 3.** Immunohistochemistry of the nodule. All spindle cells are positive for  $\alpha$ -SMA (A). There is a lumen lined by factor VIII-related antigen-positive endothelial cells (arrow) inside of the elastic fiber ring (between arrowheads). Insertion shows the same region stained with EVG staining (the same as Fig. 2A) (B). PCNA-positive cells were few in any constituent cells of the nodule including the spindle cells (C). Bars indicate 200  $\mu$ m (A) and 50  $\mu$ m (B and C).

**Disclosure of Potential Conflicts of Interest:** The authors declare no potential conflicts of interest regarding the research, authorship, or publication of this article.

**Acknowledgment:** We thank Mses. Tomomi Tajima, Yukie Sakano, Chizuko Tomiyama, Kayoko Iijima, Junko Fukumori, Takako Kazami, Mutsumi Kumagai, and Mr. Satoshi Akema for their assistance with tissue section preparation.

## References

1. The Japanese College of Veterinary Pathology. General Animal Pathology, 3rd. ed Bun-eido, Tokyo. 2013 (in Japanese).
2. Maxie MG, Jubb KVF, Kennedy PC, and Palmer N. Jubb, Kennedy, and Palmer's Pathology of Domestic Animals, 6th ed. Elsevier, 2016.
3. Adkison DL, and Sundberg JP. "Lipomatous" hamartomas and choristomas in inbred laboratory mice. *Vet Pathol.* **28**: 305–312. 1991. [Medline] [CrossRef]
4. Yamada T, Toyoda T, Ide T, Matsushita K, Morikawa T, and Ogawa K. Neuromuscular and vascular hamartoma of the small intestine in an F344 rat. *J Toxicol Pathol.* **34**: 113–117. 2021. [Medline] [CrossRef]
5. Shirota M, Kawashima J, Nakamura T, Ogawa Y, Kamiie J, and Shirota K. Vascular hamartoma in the uterus of a female Sprague-Dawley rat with an episode of vaginal bleeding. *Toxicol Pathol.* **41**: 1011–1015. 2013. [Medline] [CrossRef]
6. Sasaki T, Yoshizawa K, Kinoshita Y, Miki H, Kimura A, Yuri T, Uehara N, and Tsubura A. Spontaneously occurring intracranial lipomatous hamartoma in a young BALB/c mouse and a literature review. *J Toxicol Pathol.* **25**: 179–182. 2012. [Medline] [CrossRef]
7. Osborne JC, and Troutt HF. A congenital pulmonary anomaly (hamartoma) in a seven-month-old bovine fetus. *Cornell Vet.* **67**: 222–228. 1977. [Medline]
8. Takahashi K, Maeda K, Nakamura S, Fujita M, Orima H, Tagawa M, Kuwahara M, Nakashima N, and Maita K. Pulmonary microcystic hamartoma in an adult dog. *Vet Pathol.* **37**: 499–501. 2000. [Medline] [CrossRef]
9. Xiao S, Lux ML, Reeves R, Hudson TJ, and Fletcher JA. HMG(I)Y activation by chromosome 6p21 rearrangements in multilineage mesenchymal cells from pulmonary hamartoma. *Am J Pathol.* **150**: 901–910. 1997. [Medline]
10. WHO Classification of Tumours Editorial Board. WHO Classification of Tumours, 5th ed, Vol. 5. International Agency for Research on Cancer, Lyon. 2021.
11. Lundeen KS, Raj MS, Rajasurya V, and Ludhwani D. Pulmonary Hamartoma. 2022, from StatPearls Publishing website: <https://www.ncbi.nlm.nih.gov/books/NBK539806/>.
12. Ichiki Y, Kawasaki J, Hamatsu T, Suehiro T, Shibuya R, Matsuyama A, Tanaka F, Hisaoka M, and Sugimachi K. A rare pulmonary hamartoma: fibroleiomyomatous hamartoma. *Surg Case Rep.* **2**: 53. 2016. [Medline] [CrossRef]
13. Kato N, Endo Y, Tamura G, and Motoyama T. Multiple pulmonary leiomyomatous hamartoma with secondary ossification. *Pathol Int.* **49**: 222–225. 1999. [Medline] [CrossRef]
14. Itoh H, Yanagi M, Setoyama T, Shirao K, Yanagi S, Kataoka H, Shimotakahara T, and Koono M. Solitary fibroleiomyomatous hamartoma of the lung in a patient without a pre-existing smooth-muscle tumor. *Pathol Int.* **51**: 661–665. 2001. [Medline] [CrossRef]
15. Moroki T, Matsuo S, Hatakeyama H, Hayashi S, Matsumoto I, Suzuki S, Kotera T, Kumagai K, and Ozaki K.

- Databases for technical aspects of immunohistochemistry: 2021 update. *J Toxicol Pathol.* **34**: 161–180. 2021. [[Medline](#)] [[CrossRef](#)]
16. Gocho K, Kimura T, Hamanaka N, Ishii T, Takemura T, and Shimizu K. Airway-centered interstitial fibrosis involving smooth muscle hyperplasia with severe pulmonary hypertension. *Intern Med.* **59**: 2029–2034. 2020. [[Medline](#)] [[CrossRef](#)]
  17. Tudor RM. Pulmonary vascular remodeling in pulmonary hypertension. *Cell Tissue Res.* **367**: 643–649. 2017. [[Medline](#)] [[CrossRef](#)]
  18. Raboudi A, and Litaïem N. Congenital smooth muscle hamartoma. 2023, StatPearls Publishing. website: <https://www.ncbi.nlm.nih.gov/books/NBK545188/>.
  19. Schrom KP, Shah SD, and Rohr BR. Clinicopathologic discordance: congenital smooth muscle hamartoma clinically mimics reticulated vascular lesion. *JAAD Case Rep.* **26**: 9–12. 2022. [[Medline](#)] [[CrossRef](#)]
  20. Liu SM, and Mikaelian I. Cutaneous smooth muscle tumors in the dog and cat. *Vet Pathol.* **40**: 685–692. 2003. [[Medline](#)] [[CrossRef](#)]
  21. Schittny JC. Development of the lung. *Cell Tissue Res.* **367**: 427–444. 2017. [[Medline](#)] [[CrossRef](#)]
  22. Yamada T, Suzuki E, Gejyo F, and Ushiki T. Developmental changes in the structure of the rat fetal lung, with special reference to the airway smooth muscle and vasculature. *Arch Histol Cytol.* **65**: 55–69. 2002. [[Medline](#)] [[CrossRef](#)]